Proton Spin Relaxation Study of Molecular Motions in the Lyotropic Liquid Crystalline System Potassium-Laurate Water

W. Kühner, E. Rommel, and F. Noack
Physikalisches Institut der Universität Stuttgart

P. Meier
Institut für Physikalische Chemie der Universität Stuttgart

Z. Naturforsch. **42 a,** 127–135 (1987); received November 11, 1986

The paper presents and discusses measurements of the proton spin T_1 relaxation dispersion over a broad frequency range (100 Hz–300 MHz) in the micellar, hexagonal, cubic and lamellar phases of lyotropic potassium-laurate water mixtures. The results clearly show that in the anisotropic phases (hexagonal, lamellar) T_1 at low Larmor frequencies is dominated by liquid crystalline order fluctuations, whereas this relaxation mechanism is negligible or absent in the isotropic phases (micellar, cubic). At medium and high Larmor frequencies the relaxation reflects rotational and translational molecular motions. Using theoretical models from the literature for the three kinds of reorientations the observed frequency and temperature dependences of T_1 can be described quantitatively. In contrast to the order fluctuation mechanism the rotational and translational reorientations of individual molecules depend only weakly on the mesogenic structure. The order fluctuation contribution is strongest for the lamellar phase.

1. Introduction

Though the molecular organization and motion in lyotropic liquid crystals have been studied frequently by NMR techniques [1], the nature of the processes seen by such experiments is not understood exactly, particularly in the slow motion regime. This applies even to the most extensively investigated lyotropic system, namely the mixture of potassium-laurate $CH_3(CH_2)_{10}CO_2K$ with water, which exhibits a variety of liquid crystalline mesophases following changes of either the concentration or the temperature. The phase diagram includes a lamellar, a cubic, a hexagonal and a micellar structure [2].

Based on temperature and frequency dependent measurements of the longitudinal proton spin relaxation times T_1 and $T_{1\varrho}$ relative to a stationary or rotating Zeeman field, respectively, Charvolin et al. [1, 3] essentially separated for some mesophases three kinds of molecular reorientations with very distinct time scales: A fast hopping by self-diffusion (10^{-9} s), a strongly hindered rotation of individual molecules about their short axes (10^{-8} s), and a rather slow, long-wavelength chain deformation (10^{-6} s), which was supposed to be some kind of pendulum motion. However, since the techniques used to study the relaxation dispersion only allowed work at conventional NMR frequencies, that means over a much too restricted range with a large gap between the direct T_1 and indirect $T_{1\varrho}$ approach [4], the authors emphasized that their experimental data were insufficient for a quantitative evaluation of the various molecular reorientations.

This paper presents and discusses new measurements of the proton spin T_1 relaxation dispersion in the liquid crystalline mesophases of potassium-laurate water mixtures over a much broader Larmor frequency range (100 Hz–300 MHz) than previous works [1]. Such an improvement has become possible by taking advantage of modern field-cycling facilities [4], which eliminate the restriction of familiar NMR experiments to high Zeeman fields. The results obtained at low and medium frequencies (100 Hz–100 kHz) give clear evidence that the slow molecular tumbling in the anisotropic phases (lamellar, hexagonal) is completely different from the reorientation in the isotropic phases (cubic, micellar); in the first case

---

Reprint requests to Prof. Dr. F. Noack, Physikalisches Institut, Universität Stuttgart, Pfaffenwaldring 57, D-7000 Stuttgart 80.

0340-4811 / 87 / 0200-0127 $ 01.30/0. – Please order a reprint rather than making your own copy.

there exist smectic-type order fluctuations [5], in the second case this cooperative process is absent or negligible. As a consequence the high-frequency relaxation dispersion (10 MHz – 300 MHz) has a much more complex meaning than previously concluded in the literature [1]. It reflects both rotational and translational molecular reorientations, which differ only slightly in time scale for all considered liquid crystalline structures.

2. Experimental Techniques and Results

2.1. Sample Preparation

Potassium laurate (PL) was prepared from commercial potassium carbonate and lauric acid (Merck) applying standard techniques described in the literature [6, 7]. After removal of crystal water by drying under vacuum and purification through recrystallization from ethanol solution, one obtains the desired lyotropic mesophases by mixing the salt with water in weighed quantities according to the phase diagram [2]. Heavy water, D_2O, instead of normal water was used to distinguish solvent from solute proton spins in the NMR experiments. In order to accelerate the mixing process in the extremely viscous liquids as well as to homogenize the mixtures, it proves very helpful to centrifuge the materials and to treat them by ultrasound for several hours [7]. The exact D_2O concentrations were selected in such a way as to allow measurements of all lyotropic structures at the same temperature, and to enable a direct comparison with the data of Charvolin [3]. This meant 28 wt% for the lamellar phase, 36 wt% for the cubic phase, 50 wt% for the hexagonal phase, and 83 wt% for the micellar phase. With the help of microlitre pipettes the relative D_2O content in the NMR tubes could be adjusted to the required value with an accuracy better than 0.5%. Such a satisfactory reproducibility is significant because relaxation dispersion studies necessitate equivalent samples of different size. In the following the four considered lyotropic systems will be designated by PL 28, PL 36, PL 50 and PL 83, respectively.

2.2. NMR Apparatus

The shown measurements of the longitudinal proton relaxation time T_1 as a function of Larmor frequency ν and temperature ϑ were performed by means of three complementary NMR spectrometers operating in different frequency ranges: From zero up to 2 MHz using a home-built fast field-cycling device [8a], between 2 MHz and 80 MHz using a home-built frequency variable pulsed spectrometer [8b], and at 300 MHz with a commercial Bruker machine CXP-300 [8c]. Details about the underlying field-cycles, pulse programs, data processing and temperature control have been described previously [4, 8]. As a rule the random error of the computer assisted T_1 evaluation could be reduced to less than ± 8% by averaging both the signal amplitudes and the decay functions up to 10 times. Our apparatus allowed us to observe the relaxation dispersion essentially with one sample size (1 cm^3, 1 cm ∅), only the 300 MHz samples (0.2 cm^3, 0.5 cm ∅) had to be prepared separately. To check the equivalent composition in this case we compared T_1 at 68 MHz. Measurements at frequencies lower than approximately 300 Hz revealed a surprisingly large experimental scatter because of difficulties to compensate the earth's field exactly and to avoid fields from eddy currents; they will not be considered in this paper.

2.3. Results

Figure 1 illustrates the *frequency dependent T_1 measurements* for the individual mesophases at

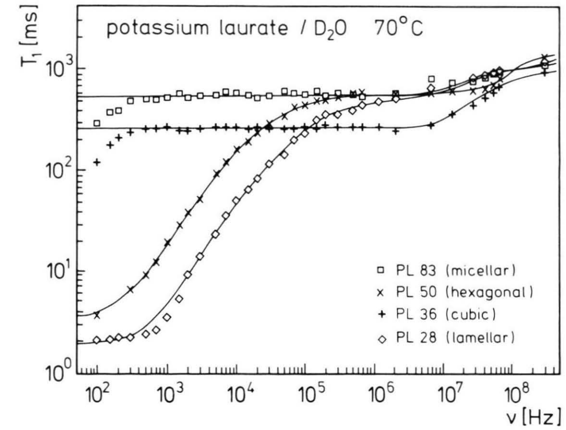

Fig. 1. T_1 proton spin relaxation dispersion in the lyotropic phases of potassium-laurate D_2O mixtures at 70 °C. The water component was adjusted to 83 wt% for the micellar phase, to 50 wt% for the hexagonal phase, to 36 wt% for the cubic phase, and to 28 wt% for the lamellar phase. The full lines are curve fits of (2) using the model parameters listed in Table 2.

70 °C. The Larmor frequency variation by a factor of $3 \cdot 10^6$ involves changes of the relaxation times by almost three orders of magnitude, and obviously the most striking effects occur outside the range of conventional spectrometers. Qualitatively, one can distinguish three regimes with quite different properties:

(i) At small frequencies ($\nu \lesssim 100$ kHz) the anisotropic mesophases (lamellar, hexagonal) show a strong dispersion of T_1, namely $T_1 \sim \nu^1$, whereas for the isotropic phases (cubic, micellar) a significant dispersion does not exist. A comparison for constant ν gives $T_1(\text{mic}) > T_1(\text{cub}) \gg T_1(\text{hex}) > T_1(\text{lam})$.

(ii) At medium frequencies ($100\text{ kHz} \lesssim \nu \lesssim 10$ MHz) there develops a plateau of T_1 both for the anisotropic and the isotropic phases, i.e. the dispersion vanishes. In this range one finds $T_1(\text{hex}) \approx T_1(\text{lam}) \approx T_1(\text{mic}) > T_1(\text{cub})$.

(iii) At high frequencies ($\nu \gtrsim 20$ MHz) the T_1 plots of all studied samples look very similar, i.e. $T_1(\text{hex}) \approx T_1(\text{lam}) \approx T_1(\text{mic}) \approx T_1(\text{cub})$. Up to the highest available values the dispersion is small, but non-negligible.

Most of these observations are in qualitative agreement with T_1 and $T_{1\varrho}$ results known in the literature [1, 3], in particular the distinction of three relaxation regimes and, consequently, of three kinds of underlying molecular motions. However, a quantitative comparison reveals significant deviations in the low-frequency range. Figure 2, which includes Charvolin's measurements of the lamellar and hexagonal phase, clearly demonstrates that the low-field T_1 dispersion is much weaker ($T_1 \sim \nu^1$) than the corresponding asymptotic $T_{1\varrho}$ behaviour ($T_{1\varrho} \sim \nu^2$). Obviously, the indirect rotating frame approach to slow time scales in NMR is not just the extension of $T_1(\nu)$ as generally assumed!

To obtain more details on the three distinct relaxation regimes, we performed additional *temperature dependent T_1 studies* at Larmor frequencies characteristic of the three cases. The results at temperatures between 30 °C and 110 °C are summarized in Figs. 3 and 4, where one should note the following:

(i) The slope of the T_1 plots as a function of temperature ϑ greatly varies when the Larmor frequency is reduced. This variation is different for the anisotropic structures (lamellar, hexagonal) from the isotropic structures (micellar, cubic); in the first case the slope decreases, in the second case it increases. Furthermore, in the isotropic phases the temperature dependence at medium and low frequencies is identical within experimental error, in contrast to the finding for the anisotropic phases.

(ii) Near 40 °C there exist discontinuities in the $T_1(\vartheta)$ plots, in particular at the lowest Larmor fre-

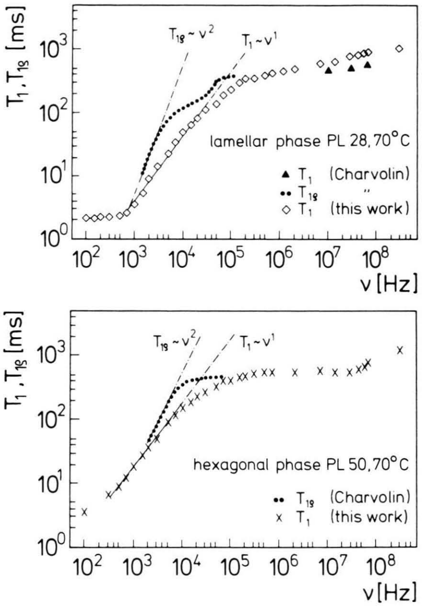

Fig. 2. Comparison of the T_1 proton spin relaxation dispersion in potassium-laurate D_2O mixtures with $T_{1\varrho}$ measurements from the literature [3d]. *Top:* Lamellar phase. *Bottom:* Hexagonal phase.

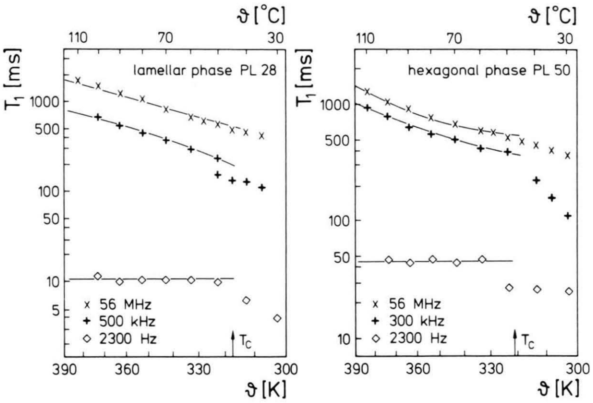

Fig. 3. Temperature dependence of the proton spin relaxation time T_1 in the anisotropic mesophases of potassium-laurate D_2O mixtures at high, medium and low Larmor frequency. *Left:* Lamellar phase. *Right:* Hexagonal phase. Note that the temperature axis is linear in $1/\vartheta$. The transition temperature to the gel state is indicated by T_c [2].

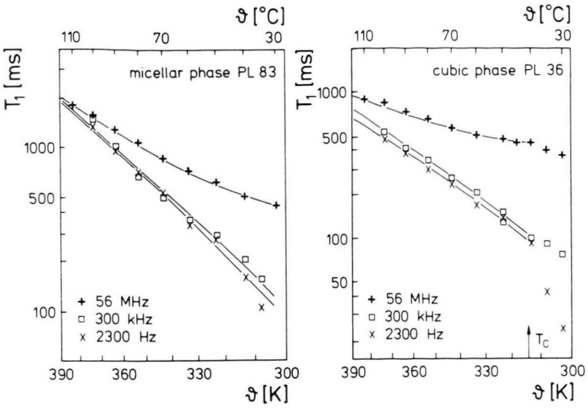

Fig. 4. Temperature dependence of the proton spin relaxation time T_1 in the isotropic mesophases of potassium-laurate D_2O mixtures at high, medium and low Larmor frequency. *Left:* Micellar phase. *Right:* Cubic phase.

quency. They indicate the transition to the gel state of the mixtures [2], which is not sharp because of hysteresis effects.

(iii) All high-frequency plots show a tendency to develop a shallow $T_1(\vartheta)$ minimum. Most likely the gel transition prevents this trend to become visible in the other curves.

Clearly, the occurrence of unlike $T_1(\vartheta)$ slopes qualitatively supports the concept that (at least) three motional processes contribute to the observed relaxation dispersion, since there exist systematic correlations between the frequency and temperature dependences. In addition, the conspicuous distinctions between the isotropic and anisotropic samples imply that the slowest of these mechanisms disappears in the micellar and cubic state. Somewhat surprisingly the board frequency variation involves only one single $T_1(\vartheta)$ minimum, namely in the high-field limit. This high-field T_1 behaviour is in excellent agreement with Charvolin's previous work [1, 3]; on the contrary, the low-field T_1 data considerably deviate from the related $T_{1\varrho}$ results [1, 3], which are not only stronger frequency dependent as shown in Fig. 2, but also much stronger temperature dependent.

3. Discussion and Conclusions

3.1. The Model

By means of computer fitting techniques it proved possible to describe the extensive new $T_1(\nu, \vartheta)$ measurements quantitatively in terms of available theoretical models on nuclear spin relaxation in liquids. Our model essentially follows Charvolin's qualitative arguments [3] that very slow oscillatory, slow rotational and fast translational molecular reorientations contribute to the proton relaxation in potassium-laurate water mixtures. However, the rich experimental details exclude an acceptable interpretation based on this concept without considerable modifications, which for instance explain the linear $T_1(\nu)$ dispersion at low Larmor frequencies and the extremely shallow $T_1(\vartheta)$ minimum at high frequencies. Such anomalies are also known in the field of thermotropic liquid crystals like MBBA, and there exists a far-reaching similarity between the results of this work and the findings in thermotropic mesogens [4, 9]. Therefore we make use of the theoretical refinements developed for thermotropics, though even this approach should be considered as a rough approximation in view of the more complex molecular structures of lyotropic mesogens.

For thermotropic systems it is now well-established that the total proton spin relaxation rate (T_1^{-1}) originates from the superposition of at least three processes, namely relaxation by

(i) oscillatory fluctuations of the liquid crystalline order with time constant $T_{1\,\mathrm{OF}}$ [5],

(ii) anisotropic rotation of individual molecules with time constant $T_{1\,\mathrm{Rot}}$ [10], and

(iii) approximately isotropic molecular self-diffusion with time constant $T_{1\,\mathrm{SD}}$ [11].

Neglecting possible correlations and with restriction to exponential relaxation this superposition is expressed by

$$\frac{1}{T_1(\nu, \vartheta)} = \frac{1}{T_{1\,\mathrm{OF}}} + \frac{1}{T_{1\,\mathrm{Rot}}} + \frac{1}{T_{1\,\mathrm{SD}}}, \qquad (1)$$

where the three contributions $1/T_{1\,\mathrm{OF}}$, $1/T_{1\,\mathrm{Rot}}$ and $1/T_{1\,\mathrm{SD}}$ differ characteristically by their Larmor frequency and temperature dependences. Table 1 summarizes the details of Eq. (1) considered to interpret the experimental results for the lyotropic potassium-laurate systems. Cross terms are disregarded in view of the unlike time scales of the underlying motions, and the assumption of exponentiality is justified by the circumstance that the total decay rate shows no deviations. Furthermore one should note that the isotropic approximation of the self-diffusion term is reasonable because the

Table 1. Model relations of the individual relaxation contributions in (1), namely for smectic liquid crystalline order fluctuations [5], for anisotropic rotation of single molecules [10], and for isotropic molecular self-diffusion [11]. The notation essentially follows the original papers, but makes use of SI units. μ_0: magnetic permeability of vacuum; γ: proton magnetogyric ratio; $\hbar = h/2\pi$: Planck's constant divided by 2π; ϑ: absolute temperature; ν: proton Larmor frequency; R: gas constant.

$T_{1\mathrm{OF}}$ *term.* a: effective proton-proton separation; φ_a: effective proton pair orientation; k: Boltzmann's constant; S: liquid crystalline order parameter; K_{el}: average elastic constant; ξ: coherence length; ν_{loc}: low-field dispersion cut-off frequency.

$T_{1\mathrm{Rot}}$ *term.* b: effective proton-proton separation; φ: effective proton pair orientation; $\tau_\parallel$: time constant of reorientations about the long molecular axis; $\tau_\perp$: time constant of reorientations about the short molecular axes (Woessner writes $T_{1\mathrm{Rot}}$ in terms of the rotational diffusion constants $R_1 = 1/\tau_\parallel$ and $R_2 = 1/\tau_\perp$ [10]); $\tau_\parallel^0$, $\tau_\perp^0$, $E_\parallel$, $E_\perp$: related preexponential factors and activation energies of Arrhenius laws.

$T_{1\mathrm{SD}}$ *term.* N_{p}: local proton spin density; c: distance of closest intermolecular proton-proton approach; τ_t: time constant of translational molecular jumps; τ_t^0, E_t: related preexponential factor and activation energy.

Reorientation	Relaxation rate
Smectic order fluctuations	$\frac{1}{T_{1\mathrm{OF}}} = \left[\frac{\mu_0}{4\pi}\right]^2 \frac{9}{8} \gamma^4 \hbar^2 \frac{k\,\vartheta\,S^2}{4K_{\mathrm{el}}\,\xi} \frac{(3\cos^2\varphi_a - 1)^2}{4a^6} \frac{1}{(\nu^2 + \nu_{\mathrm{loc}}^2)^{1/2}} \equiv A(\vartheta, S, K_{\mathrm{el}}, \varphi_a, a)\; f_{\mathrm{OF}}(\nu, \nu_{\mathrm{loc}})$ with $A = \mathrm{const}(\vartheta)$
Anisotropic molecular rotation	$\frac{1}{T_{1\mathrm{Rot}}} = \left[\frac{\mu_0}{4\pi}\right]^2 \frac{9}{8} \gamma^4 \hbar^2 \frac{4}{15b^6}$ $\cdot \sum_{p=1}^{2} p^2 \left[\frac{3}{24} \frac{(3\cos^2\varphi - 1)^2 \tau_\perp}{1 + (p\,\pi\,\nu\,\tau_\perp/3)^2} + \frac{3}{4} \frac{\sin^2(2\varphi)\,\tau_\parallel}{1 + (p\,2\pi\,\nu\,\tau_\parallel)^2} + \frac{3}{16} \frac{\sin^4\varphi\,\tau_\parallel}{1 + (p\,\pi\,\nu\,\tau_\parallel/2)^2}\right]$ $\equiv B(b)\; f_{\mathrm{Rot}}(\nu, \tau_\perp, \tau_\parallel, \varphi)$ with $B = \mathrm{const}(\vartheta)$, $\varphi = \mathrm{const}(\vartheta)$, $\tau_\perp = \tau_\perp^0 \exp(E_\perp/R\vartheta)$, $\tau_\parallel = \tau_\parallel^0 \exp(E_\parallel/R\vartheta)$
Self-diffusion	$\frac{1}{T_{1\mathrm{SD}}} = \left[\frac{\mu_0}{4\pi}\right]^2 \frac{9}{8} \gamma^4 \hbar^2 \frac{32\pi N_{\mathrm{p}}}{5c^3}$ $\cdot \sum_{p=1}^{2} p^2 \frac{\tau_t}{x^4} \left[\frac{x}{2} - \frac{1}{x} - \exp(-x)\left[\left[\frac{x}{2} - \frac{1}{x}\right]\sin x + \left[\frac{x}{2} + \frac{1}{x} + 2\right]\cos x\right]\right]$ $\equiv C(N_{\mathrm{p}}, c)\; f_{\mathrm{SD}}(\nu, \tau_t)$ with $x \equiv (p\,12\pi\,\nu\,\tau_t)^{1/2}$, $C = \mathrm{const}(\vartheta)$, $\tau_t = \tau_t^0 \exp(E_t/R\,\vartheta)$

anisotropy of the self-diffusion constant in liquid crystals is surprisingly small, where data are available, and its effect on T_1 was unobservable so far [12].

The mathematical relations listed in Table 1 demonstrate why measurements of the relaxation dispersion are essential in order of study molecular reorientations by T_1: Whereas the frequency dependence, $T_1(\nu)$, is very transparent and thus easily makes possible to disentangle a superposition of processes, the temperature dependence, $T_1(\vartheta)$, may be extremely complex due to the numerous quantities involved, which generally prevents the evaluation of individual model parameters. In the present case the $T_1(\vartheta)$ data are primarily used to test if the model, obtained from the dispersion plots at constant temperature, can be made compatible with the temperature dependent results at constant frequency. For simplicity we take into account only variations caused by the thermally activated reorientation processes, which most likely dominate the properties of $T_1(\vartheta)$, and neglect potential effects due to changes of the molecular structure. A detailed separation of the individual temperature dependences of the underlying structural elements, such as the interspin separation, orientation or order parameter, is not possible solely by T_1 measurements.

3.2. Curve Fitting

The theoretical curves drawn in Figs. 1, 3 and 4 were calculated by evaluating the expressions of Table 1 with the help of a IBM Personal Computer, and then successively optimizing all model parameters so that the deviations between the experimental data points and the theoretical predictions vanished or became small compared with the experimental scatter. For the fitting procedure Eq. (1) is suitably rewritten in the form

$$T_1^{-1} = A f_{\mathrm{OF}}(\nu, \nu_{\mathrm{loc}}) + B f_{\mathrm{Rot}}(\nu, \tau_\perp, \tau_\parallel, \varphi) + C f_{\mathrm{SD}}(\nu, \tau_t), \tag{2}$$

which explicitly shows the different kinds of adjustable model constants in the dispersion law $T_1(\nu)$, namely intensity factors A, B, C, motional time constants $\tau_\perp$, $\tau_\parallel$, τ_t, the low frequency cut-off ν_{loc}, and the spin pair orientation φ. Details of this notation are given in Table 1. The amplitudes A, B, C of the three relaxation terms have to be treated as adjustable parameters because the microscopic distances, angles, lengths and densities which govern these quantities are not known for potassium-laurate systems. Note the most helpful circumstance that these amplitudes, unlike all other fitting constants, linearly depend on the relaxation rate. Once $T_1(\nu)$ has been optimized, the related evaluation of $T_1(\vartheta)$ is not only a means to observe changes of the molecular structure and dynamics, but also a critical method to eliminate ambiguities of the analysis. However, any temperature dependence included in Eq. (2) by additional model relations complicates the fit so that at the moment approximations are indispensable. Based on the arguments of Sect. 3.1, we considered only the reorientation times by assuming the Arrhenius laws

$$\tau_\perp = \tau_\perp^0 \exp(E_\perp / R\vartheta), \tag{3a}$$

$$\tau_\parallel = \tau_\parallel^0 \exp(E_\parallel / R\vartheta), \tag{3b}$$

$$\tau_t = \tau_t^0 \exp(E_t / R\vartheta) \tag{3c}$$

with preexponentials $\tau_\perp^0$, $\tau_\parallel^0$, τ_t^0 and activation energies $E_\perp$, $E_\parallel$, E_t as new fitting constants.

Despite the numerous model coordinates the procedure always led to a definite solution if both $T_1(\nu)$ and $T_1(\vartheta)$ were interpreted by the same set of parameters, and if the translational jumping time τ_t was made compatible with measurements of the self-diffusion constant [13]. This restriction increases the importance of the rotational compared with the translational relaxation term, and thus allows to determine the two rotational jumping times $\tau_\perp$, $\tau_\parallel$ with better accuracy. Examples of the individual contributions to $T_1(\nu)$ and $T_1(\vartheta)$ are illustrated in Figs. 5 and 6, the complete results are listed in Table 2. Roughly speaking, A and ν_{loc} describe the dispersion at low frequencies, C, τ_t and $\tau_\parallel$ are responsible for the high-frequency range, whilst B,

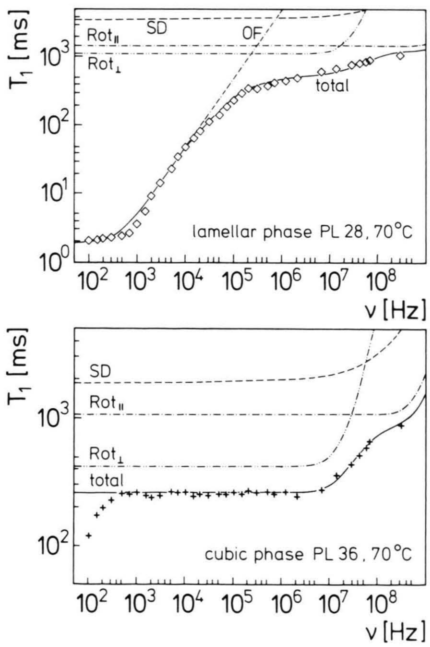

Fig. 5. Illustration of the individual relaxation contributions in potassium-laurate D_2O mixtures obtained from the curve fit of (2) to the relaxation dispersion measurements shown in Figure 1. *Top:* Lamellar phase. *Bottom:* Cubic phase. For details see text.

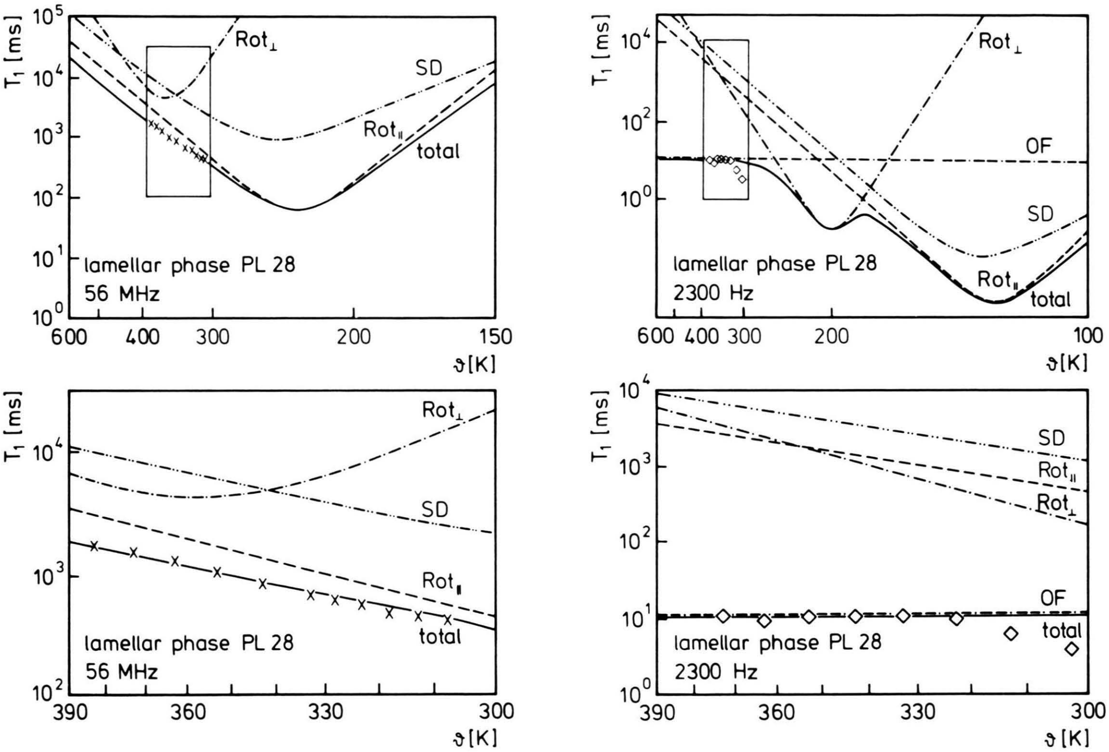

Fig. 6. Illustration of the individual relaxation contributions in potassium-laurate D_2O mixtures obtained from the curve fit of (2) and (3) to the temperature dependent measurements shown in Figure 3. *Right:* Lamellar phase, low frequency regime. *Left:* Lamellar phase, high frequency regime. The temperature axes are linear in $1/\vartheta$. Note from the extensions of the calculations to temperatures below the proper mesophase range (top) that the relaxation minima due to molecular rotations and self-diffusion are observable only at very high Larmor frequencies, where the maximum relaxation rates shift to higher temperatures. In contrast to conclusions in the literature [3] the process responsible for the T_1 minimum detectable near 100 MHz is the slow molecular tumbling about the short axis (Rot$_\perp$) and not the much faster self-diffusion (SD). For details see text.

Table 2. Model parameters obtained by curve fits of (2) to the experimental proton spin relaxation in micellar, hexagonal, cubic and lamellar potassium-laurate D_2O mixtures.

Model parameters	Micellar phase PL 83	Hexagonal phase PL 50	Cubic phase PL 36	Lamellar phase PL 28
A/s^{-2}	0	$5.1 \cdot 10^4$	0	$2.1 \cdot 10^5$
$\nu_{\mathrm{loc}}/\mathrm{Hz}$	–	165	–	400
B/s^{-2}	$3.6 \cdot 10^9$	$2.1 \cdot 10^9$	$2.2 \cdot 10^9$	$3.6 \cdot 10^9$
$\tau_\parallel$ (70 °C)/s	$5.0 \cdot 10^{-11}$	$5.0 \cdot 10^{-11}$	$8.0 \cdot 10^{-11}$	$4.0 \cdot 10^{-11}$
$\tau_\perp$ (70 °C)/s	$4.0 \cdot 10^{-9}$	$8.0 \cdot 10^{-10}$	$4.1 \cdot 10^{-9}$	$3.0 \cdot 10^{-9}$
$E_\parallel/\mathrm{kJ\,mol^{-1}}$	22	8	14	22
$\tau_\parallel^0/\mathrm{s}$	$2.2 \cdot 10^{-14}$	$3.0 \cdot 10^{-12}$	$5.9 \cdot 10^{-13}$	$1.8 \cdot 10^{-14}$
$E_\perp/\mathrm{kJ\,mol^{-1}}$	43	30	35	38
$\tau_\perp^0/\mathrm{s}$	$1.1 \cdot 10^{-15}$	$2.1 \cdot 10^{-14}$	$1.9 \cdot 10^{-14}$	$4.9 \cdot 10^{-15}$
$\varphi/°$	44	27	34	41
C/s^{-2}	$3.0 \cdot 10^7$	$8.2 \cdot 10^9$	$9.5 \cdot 10^9$	$7.0 \cdot 10^9$
τ_t (70 °C)/s	$1.8 \cdot 10^{-9}$	$1.4 \cdot 10^{-10}$	$1.7 \cdot 10^{-10}$	$1.2 \cdot 10^{-10}$
$E_t/\mathrm{kJ\,mol^{-1}}$	30	20	22	22
τ_t^0/s	$4.7 \cdot 10^{-14}$	$1.2 \cdot 10^{-13}$	$7.6 \cdot 10^{-14}$	$5.4 \cdot 10^{-14}$

$\tau_\perp$ and φ govern the transition regime. Note from the diagrams that with the exception of the $\tau_\perp$ process the characteristic rotational and translational $T_1(\vartheta)$ minima appear at temperatures where the mesophases no longer persist. Systematic variations of the model parameters are disclosed for all three relaxation terms, but only the order fluctuation contribution exhibits dramatic changes.

3.3. *Interpretation*

On the basis of Charvolin's pioneering work [3] our analysis demonstrates that the motionally induced proton spin relaxation in a simple binary lyotropic system can be interpreted quantitatively. Two aspects of the model fit by means of three kinds of molecular motions are of particular importance:

(i) The slow reorientation in the lamellar and hexagonal phase is a cooperative mechanism, namely a thermally generated overdamped oscillation of the director field (director order fluctuations). This process is more effective in the lamellar than in the hexagonal phase, and it is completely absent in the cubic and micellar phase where the director is not defined.

(ii) The translational and rotational reorientations of individual molecules depend only weakly on the mesogenic structure. Most obvious are the increased activation barriers in the micellar sample.

What do we learn from the related numbers in Table 2 about the geometry and dynamics of the potassium molecules? Let us consider the three processes separately.

The amplitude factor of the order fluctuation term, A, differs between the lamellar phase and the hexagonal phase by a factor 21/5.1 = 4.1. According to the model relation

$$A = \left[\frac{\mu_0}{4\pi}\right]^2 \frac{9}{8}\gamma^4 \hbar^2 \frac{1}{a^6} \frac{(3\cos^2\varphi_a - 1)^2}{4} \frac{k\vartheta S^2}{4K_{\mathrm{el}}\,\xi}, \tag{4}$$

the observed variation may be attributed to changes of the proton-proton separation a, the protonp air orientation φ_a, the order parameter S, the elastic constant K_{el} or the coherence length ξ. Surprisingly, the effect can be described wholly by S [14], because the molecules in the lamellar state align approximately parallel to the director ($S \cong 1$), whereas in the hexagonal state they align perpendicular to this axis ($S \cong -1/2$). Consequently, if one puts $a = b$, $\varphi_a = \varphi$ and makes use of the values for b and φ derived from the rotational contribution, Eq. (4) implies $K_{\mathrm{el}}\,\xi\,(\mathrm{lam}) = 1.0 \cdot 10^{-17}\,\mathrm{N\,m}$ and $K_{\mathrm{el}}\,\xi\,(\mathrm{hex}) = 2.1 \cdot 10^{-17}\,\mathrm{N\,m}$, and thus allows to estimate the magnitude of ξ. With the assumption that K_{el} is comparable to the splay constant of typical thermotropic liquid crystals, i.e. $K_{\mathrm{el}} \cong 5.0 \cdot 10^{-12}\,\mathrm{N}$ [15], one obtains $\xi\,(\mathrm{lam}) \cong 2.0 \cdot 10^{-6}\,\mathrm{m}$ and $\xi\,(\mathrm{hex}) \cong 4.3 \cdot 10^{-6}\,\mathrm{m}$, respectively. This is about 100 to 200 times the length of the potassium molecule ($17 \cdot 10^{-8}\,\mathrm{m}$) and of the same order as experimental results for nematics [16]. The estimation reveals that in both cases the cut-off frequency of the relaxation dispersion, ν_{loc}, is determined by internal dipolar fields and not by the longest order fluctuation mode, since an order fluctuation limited cut-off should entail $\nu_{\mathrm{loc}} \sim 1/\xi^2$ [5] instead of $\nu_{\mathrm{loc}}(\mathrm{lam}) > \nu_{\mathrm{loc}}(\mathrm{hex})$.

The amplitude factor of the rotational term,

$$B = \left[\frac{\mu_0}{4\pi}\right]^2 \frac{9}{8}\gamma^4 \hbar^2 \frac{4}{15 b^6}, \tag{5}$$

is slightly different for the various mesophases, and thus leads to unlike values of the average intramolecular proton-proton separation b of rotating dipole pairs: $b(\mathrm{lam}) = 1.90 \cdot 10^{-10}\,\mathrm{m}$, $b(\mathrm{cub}) = 2.07 \cdot 10^{-10}\,\mathrm{m}$, $b(\mathrm{hex}) = 2.08 \cdot 10^{-10}\,\mathrm{m}$, and $b(\mathrm{mic}) = 1.90 \cdot 10^{-10}\,\mathrm{m}$. As seen from Table 2, these variations are related to changes of the average proton pair orientation angle φ. Both observations indicate unlike conformations of the tumbling molecules. Unfortunately, our present measurements cannot discern individual spin sites and therefore do not allow to evaluate which molecular segments are responsible for the effect. Furthermore, the underlying assumption that the particles subject to rotational jumps are rigid symmetrical ellipsoids which tumble as a whole about their long and short axes with time constants $\tau_\parallel$ and $\tau_\perp$, respectively, is certainly a coarse approximation. Nevertheless, our concept is supported by dielectric relaxation studies of lyotropic systems, where one usually finds reorientation rates of similar magnitude [17]. A significant aspect is the large $\tau_\perp/\tau_\parallel$ ratio of 50−80 (70 °C) in the macroscopically isotropic phases, because it is a clear indication for the microscopically anisotropic ordering potential even in these structures. For an ellipsoid with dimensions of a potassium molecule (long axis $2a \cong 17 \cdot 10^{-10}\,\mathrm{m}$, short axis $2b \cong 5 \cdot 10^{-10}\,\mathrm{m}$, $b/a \cong 0.3$) and in an isotropic viscous surrounding this ratio should be only 19.9 [18]. The microscopic anisotropy is also seen by the unlike activation energies, $E_\perp > E_\parallel$, which means that $\tau_\perp/\tau_\parallel$ further increases at smaller temperatures.

The self-diffusion term, characterized in Table 2 by the amplitude factor

$$C = \left[\frac{\mu_0}{4\pi}\right]^2 \frac{9}{8}\gamma^4 \hbar^2 \frac{32\pi N_{\mathrm{p}}}{5c^3} \tag{6}$$

and the translational jumping time τ_t, provide the least effective relaxation mechanism as illustrated in Figure 5. This circumstance, unusually in view of the results known for nematic thermotropic liquid crystals [9], makes it difficult to determine precisely the model parameters C and τ_t or the related proton spin density N_{p} and the distance of closest intermolecular proton approach c. In the present case the problem is somewhat simplified because (i) the self-diffusion constant D of potassium-laurate mixtures, which relates c and τ_t by the Einstein relation $c^2 = 6D\tau_t$, has been measured independently [12], and because (ii) the proton spin density N_p can be estimated reliably from the number of protons per molecule, the molecular length and the area of polar head groups [3, 19]. So the curve fit essentially determines the value of c. Using for the lamellar phase $N_p = 3.56 \cdot 10^{28}\,\mathrm{m}^{-3}$, $D = 2.2 \cdot 10^{-6}\,\mathrm{cm}^2\,\mathrm{s}^{-1}$, for the cubic phase $N_p = 5.76 \cdot 10^{28}\,\mathrm{m}^{-3}$, $D = 1.8 \cdot 10^{-6}\,\mathrm{cm}^2\,\mathrm{s}^{-1}$, for the hexagonal phase $N_p = 5.10 \cdot 10^{28}\,\mathrm{m}^{-3}$, $D = 2.1 \cdot 10^{-6}\,\mathrm{cm}^2\,\mathrm{s}^{-1}$, and for the micellar phase $N_p = 5.79 \cdot 10^{28}\,\mathrm{m}^{-3}$, $D = 2.6 \cdot 10^{-6}\,\mathrm{cm}^2\,\mathrm{s}^{-1}$ (all values at 70 °C) gives $c(\mathrm{lam}) = 3.95 \cdot 10^{-10}\,\mathrm{m}$, $c(\mathrm{cub}) = 4.20 \cdot 10^{-10}\,\mathrm{m}$, $c(\mathrm{hex}) = 4.20 \cdot 10^{-10}\,\mathrm{m}$, and $c(\mathrm{mic}) = 4.29 \cdot 10^{-10}\,\mathrm{m}$, respectively. This distance is slightly less than the short diameter of the molecular ellipsoid and hence reasonable for the closest approach of two effective spins positioned at the centre of neighbouring molecules. Refinements of the self-diffusion model for the micellar state by Žumer et al. [20], which take into account translationally induced molecular rotations and thus involve a more complex reorientation time constant τ_t, could not be analysed with the available experimental data due to the presence of the dominating competing relaxation process. However, the results for τ_t and E_t in Table 2 clearly indicate that self-diffusion in the micellar phase is more strongly hindered and the jumping time is somewhat slower than in all other states.

Acknowledgements

The authors thank Prof. Dr. G. Kothe, Dr. M. Vilfan, Dipl.-Phys. K. H. Schweikert, and Mr. M. Notter for helpful comments to this work. The financial support by grants from the Deutsche Forschungsgemeinschaft is gratefully acknowledged.

[1] (a) A. Johansson and B. Lindman, in: Liquid Crystals and Plastic Crystals (G. W. Gray and P. A. Winsor, eds.), Ellis Horwood, Chichester, Vol. 2, p. 192 (1974); (b) J. Charvolin and A. Tardieu, Solid State Physics, Suppl. **14,** 209 (1978).

[2] P. Ekwall, Advances in Liquid Crystals **1,** 1 (1975).

[3] (a) J. Charvolin and P. Rigny, J. Physique **30,** C 4 (1969); (b) P. Rigny and J. Charvolin, J. Physique **32,** C 5 (1971); (c) G. Agren, J. Physique **33,** 887 (1972); (d) J. Charvolin and P. Rigny, J. Chem. Phys. **58,** 3999 (1973).

[4] F. Noack, Prog. Nuclear Magn. Reson. Spectrosc. **18,** 171 (1986).

[5] (a) R. Blinc, M. Luzar, M. Vilfan, and M. Burgar, J. Chem. Phys. **63,** 3445 (1975); (b) J. A. Marqusee, M. Warner, and K. A. Dill, J. Chem. Phys. **81,** 6404 (1984).

[6] T. R. Lomer, Acta Cryst. **5,** 11 (1952).

[7] (a) B. Furtner, Diplomarbeit, Universität Stuttgart 1980; (b) W. Kühner, Diplomarbeit, Universität Stuttgart 1986.

[8] (a) E. Rommel, K. Mischker, G. Osswald, K. H. Schweikert, and F. Noack, J. Magn. Reson. **70,** in press (1986); (b) M. Stohrer and F. Noack, J. Chem. Phys. **67,** 3729 (1977); (c) K. Müller, P. Meier, and G. Kothe, Prog. Nuclear Magn. Reson. Spectrosc. **17,** 211 (1985).

[9] (a) V. Graf, F. Noack, and M. Stohrer, Z. Naturforsch. **32a,** 61 (1977); (b) R. Blinc, M. Vilfan, M. Luzar, J. Seliger, and V. Žagar, J. Chem. Phys. **68,** 303 (1978); (c) Th. Mugele, V. Graf, W. Wölfel, and F. Noack, Z. Naturforsch. **35a,** 924 (1980).

[10] (a) D. E. Woessner, J. Chem. Phys. **37,** 647 (1962); (b) W. T. Huntress, J. Chem. Phys. **48,** 3524 (1968).

[11] H. Pfeifer, Ann. Phys. **8,** 1 (1961).

[12] (a) S. Žumer and M. Vilfan, Phys. Rev. **A 17,** 424 (1978); (b) M. Vilfan and S. Žumer, Bull. Magn. Reson. **2,** 327 (1981).

[13] (a) R. T. Roberts, Nature **242,** 348 (1973); (b) G. Chidichimo, A. Golemme, G. A. Ranieri, M. Terenzi, and J. W. Doane, Mol. Cryst. Liq. Cryst. **132,** 275 (1986).

[14] J. Charvolin and Y. Hendriks, in: Nuclear Magnetic Resonance of Liquid Crystals (J. W. Emsley, ed.), D. Reidel Publ. Comp., Dordrecht 1985, p. 449.

[15] (a) G. Durand, R. Bartolino, and M. Cagnon, Chem. Phys. **11,** 107 (1980); (b) W. H. de Jeu, Physical Properties of Liquid Crystalline Materials, Gordon and Breach, New York 1980.

[16] V. Graf, Thesis, Universität Stuttgart 1980.

[17] (a) H. Kresse, Advances in Liquid Crystals **6,** 109 (1983); (b) R. Pottel, K. D. Göpel, R. Henze, U. Kaatze, and V. Uhlendorf, Biophys. Chem. **19,** 233 (1984).

[18] P. Perrin, J. Physique Radium **5,** 497 (1934).

[19] (a) F. Husson, M. Mustacchi, and V. Luzzati, Acta Cryst. **13,** 688 (1960); (b) V. Luzzati, A. Tardieu, T. Gulik-Krzywicki, E. Rivas, and F. Husson, Nature London **220,** 485 (1968).

[20] S. Žumer and M. Vilfan, J. Physique **46,** 1763 (1985).